JOURNAL OF SOLID STATE CHEMISTRY 106, 493–500 (1993)

Chemically Prepared Fe–B Ultrafine Amorphous Alloy Particles: Influence of the Reaction Time on the Properties

JIANYI SHEN,* ZHIYU LI, YINING FAN, ZHENG HU, AND YI CHEN

Department of Chemistry, Nanjing University, Nanjing 210008, China

Received November 4, 1992; in revised form February 19, 1993; accepted February 23, 1993

Fe–B ultrafine amorphous alloys have been prepared by adding the solution of potassium borohydride into the solution of ferrous sulfate. The reaction process, monitored by the change in pH value during the reaction, and the effect of addition rate of KBH_4 solution, i.e., the reaction time, were investigated. It was found that the reaction system automatically maintains its pH value at about 4.6 and the molar ratio of KBH_4 to $FeSO_4$ for the equivalent reaction is 1.9. The boron content increased with the time used for adding 142 ml of KBH_4 solution up to about 50 min and then decreased. Generally, the particle size was smaller for high addition rate (e.g. 590 Å with 7 sec) and large for low addition rate (e. g. 1370 Å with 96 min). The amorphous structure of the Fe–B alloys was also found to be different with different reaction time used.

Introduction

Since the work of van Wonterghem *et al.* was published (*1*), the Fe–B and Fe–*M*–B (*M* = Co, Ni) ultrafine amorphous alloy particles (UFAAP) and their chemical preparation methods have been extensively studied (*2–18*). Chemical methods can be easily used for large-scale production of these materials which are expected to have applications in catalysis, magnetic recording, and ferrofluids. The Fe–B UFAAP can be produced by reduction of iron ions with borohydride in aqueous solution. The properties of the chemically prepared Fe–B UFAAP and preparation parameters such as pH, concentration, and methods of combining the reactant solutions have been reviewed (*19*). In this work, the samples of Fe–B UFAAP were prepared by adding KBH_4 solution into $FeSO_4$ solution. The reaction takes place very fast and vigorously when the two reactant solutions were mixed at room temperature. So, the addition time of KBH_4 solution is the reaction time for the reaction between $FeSO_4$ and KBH_4. The properties of the Fe–B products were found to be greatly influenced by the addition rate of KBH_4 solution, i.e., the reaction time used.

*To whom correspondence should be addressed at Chemical Engineering Department, 1415 Johnson Drive, University of Wisconsin-Madison, Madison, WI 53706.

Experimental

The Fe–B UFAAP were prepared by reacting $FeSO_4$ with KBH_4 in aqueous solution. Specifically, 142 ml of KBH_4 solution (0.49 *M*) containing 3.77650 g of KBH_4 (purity: 99%) was added into 200 ml of $FeSO_4$ solution (0.1 *M*) containing 5.56020 g of $FeSO_4 \cdot 7H_2O$ (purity: 98%) at a constant rate. A schematic of the apparatus used appears in Fig. 1. The solution of KBH_4 was first filled into a volumetric reservoir. The solution of $FeSO_4$ was put in a jacketed beaker with a stream of water at constant temperature of 293 K cycling in the outer jacket. The solution in the beaker was stirred with a magnetic stirrer. KBH_4 solution was then forced into the $FeSO_4$ solution through a

0022-4596/93 $5.00

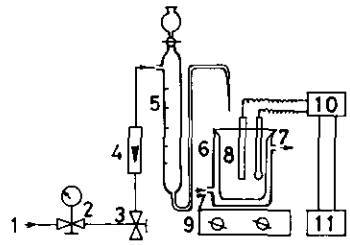

FIG. 1. A schematic diagram of the apparatus for preparing Fe–B alloys. (1) Nitrogen cylinder. (2) Pressure regulator. (3) Micro metering valve. (4) Float flow meter. (5) Volumetric reservoir. (6) Jacketed beaker. (7) Inlet and outlet for water with constant temperature from a precise water bath (±0.1 K). (8) Electrodes for measuring pH. (9) Magnetic stirrer. (10) EA-920 ion analyzer. (11) X–Y recorder.

dropper by nitrogen gas at 0.15 MPa. The flow rate of nitrogen was controlled with a micrometering valve and measured with a float flow meter. The flow rate of the solution from the volumetric reservoir was found to be approximately equal to that of nitrogen gas. The change of pH value of the solution in the beaker versus reaction process was measured by an EA-920 ion analyzer with accuracy of 0.02 pH units. The precipitates produced in the beaker during the reaction were washed thoroughly with distilled water for removal of reaction residues and then with acetone for drying. In order to prevent oxidation, the samples were soaked in acetone when transferred into a flask for passivation. The passivation usually took 24 hr in flowing nitrogen (120 ml/min) containing approximately 1% of oxygen. The samples thus prepared are stable when exposed to air.

The composition of the samples was analyzed by an inductively coupled plasma method (ICP). Mössbauer spectroscopy was used to identify the amorphous and crystalline phases of the samples. Mössbauer spectra were collected at room temperature using a ^{57}Co source in a palladium matrix and were fitted according to the method described by Le Caër and Dubois (*20*). The Mössbauer parameters were calibrated with respect to α-Fe.

The morphology and particle sizes of the samples were determined by transmission electron microscopy (TEM). The BET surface areas were also measured by the adsorption of nitrogen, from which the average particle sizes were calculated. Differential scanning calorimetry (DSC) was performed in argon with a scan rate of 20 K/min to characterize the crystallization process and heat of the samples.

Results and Discussion

We have discussed the mechanism of the reaction of Fe^{2+} with BH_4^- in aqueous solution for producing Fe–B UFAAP elsewhere (*21*). We have shown that the reaction between Fe^{2+} and BH_4^- ions is composed of the following individual reactions:

$$BH_4^- + 2H_2O \rightarrow BO_2^- + 4H_2 \quad (1)$$

$$BH_4^- + 2Fe^{2+} + 2H_2O \rightarrow 2Fe + BO_2^- + 4H^+ + 2H_2 \quad (2)$$

$$BH_4^- + H_2O \rightarrow B + OH^- + 2.5H_2 \quad (3)$$

Equation (1) represents the reaction of H^- in BH_4^- with H^+ in H_2O or the decomposition of BH_4^- in water, which is found to be unavoidable during the reaction. This reaction causes an increase of pH value of the reaction system because of the consumption of H^+ and the hydrolysis of BO_2^-. Equations (2) and (3) represent the reductions of Fe^{2+} and B^{3+} by H^- in BH_4^- respectively. The reduction of Fe^{2+} to Fe metal releases H^+, which will greatly decrease pH value of the reaction solution. Figure 2 shows the typical reaction process indicated by the change of pH versus time. The total time for adding 142 ml of KBH_4 solution is 23.45 min in this case. Because the electrode potential of H^+ ($\varnothing^0 = 0$ V) is much greater than that of Fe^{2+} ($\varnothing^0 = -0.414$ V), only reaction (1) can take place at the beginning ($t \sim 0$), which causes a sharp increase in the pH value of the reaction solution. At pH = 6.95, the reduction of Fe^{2+}, as represented by the Eq. (2), begins, which then sharply decreases

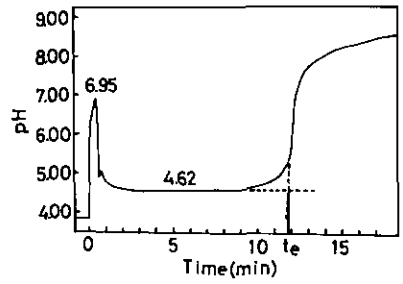

FIG. 2. The dependence of pH value of the reaction solution upon reaction process when 142 ml of 0.49 *M* KBH_4 solution was added into 200 ml of 0.1 *M* $FeSO_4$ solution in 23.45 min.

the pH of the reaction solution. Afterwards, the pH value remains almost constant at about 4.6, because either of the reactions (1) and (2), which produce OH^- and H^+ respectively, promotes its counterpart. Thus, the pH value of the reaction between $FeSO_4$ and KBH_4 in aqueous solution is automatically held at around 4.6. At time t_e, as shown in Fig. 2, the pH value sharply increases again, indicating that the Fe^{2+} ions in the solution have been completely reduced and only reaction (1) continues to proceed. According to the amount of KBH_4 used up to t_e, the molar ratio of KBH_4 to $FeSO_4$ for their equivalent reaction was found to be about 1.9. A molar ratio used exceeding this value represents an excess for borohydride reduction of Fe^{2+}.

Different rates for adding 142 ml of KBH_4 solution into 200 ml of $FeSO_4$ solution have been used to produce Fe–B samples. All the reaction processes are similar to that shown in Fig. 2. Properties of these samples are collected in Table I. Boron content, average particle sizes ($\bar{d}$), mean hyperfine fields ($\bar{H}$), and crystallization heat (ΔH_C) of the samples depend significantly on the addition rate of KBH_4 solution, i.e., the reaction time.

The room temperature Mössbauer spectra of the Fe–B samples prepared with the addition time for the 142 ml of KBH_4 solution from 7 sec to 96 min are shown in Fig. 3. The spectra of the samples with the time from 9 to 96 min are similar to each other and exhibit broadened sextets, which are characteristic of amorphous iron alloys (*19*). The spectra of the samples prepared with the time of equal to or less than 5 min exhibit even broader sextets so that the six absorption lines can not be clearly distinguished. It should be noted that the very broadening of the sextets for these three samples is not caused by impurities because the ICP analysis accounts for nearly 100% weight of the constituent elements (see Table I). This may imply that these samples have more disordered amorphous structure and/or smaller particle sizes than those samples prepared with the time longer than 5 min. In the spectrum of the sample with very fast addition rate (142 ml/7 sec), a sharp absorption sextet with a hyperfine field of 330 kOe was fitted in addition to the broad sextet of the amorphous phase. About 3% of the total spectral area can be assigned to the crystalline phase of α-Fe in this sample. For the samples prepared with the time from 2 to 5 min, the existence of α-Fe can also be observed by their Mössbauer spectra although it was not included in the fits.

In Fig. 4 are shown the dependence of boron content and mean hyperfine field of the Fe–B samples on the reaction time. The values of boron content (at.%) and mean hyperfine field ($\bar{H}$) for all the samples prepared with the reaction time from 7 sec to 96 min appear near the corresponding curves. The T7s sample prepared at the fastest addition rate (142 ml/7 sec) has the lowest boron content (10 at.%). The boron content increases with increasing the reaction time until about 50 min and then decreases. The samples prepared with the reaction time at about 50 min contain about 30 at.% of boron. The dependence of mean hyperfine field on the reaction time is the reverse of that with boron content. This strongly supports the ICP results and further confirms the linear correlation between hyperfine field and the boron content in Fe–B samples as described by Linderoth *et al.* (*19*).

Assuming that the Fe-B particles are

TABLE I

PROPERTIES OF THE Fe–B UFAAP PREPARED WITH THE DIFFERENT REACTION TIME BY ADDING 142 ml OF 0.49 *M* KBH_4 SOLUTION INTO 200 ml OF 0.1 *M* $FeSO_4$ SOLUTION

Sample	Time (min)	ICP results (wt%) Fe	B	Total	Composition (at.%)	BET area (m^2/g)	$\bar{d}$ (Å)	$\bar{H}$ (kOe)	ΔH_C (J/g)
T7s	7 sec	91.9	1.9	93.8	Fe90B10	13	590	275	83
T2	2.23	92.9	3.5	96.4	Fe84B16	11	680	270	80
T5	5.00	95.2	4.2	99.4	Fe81B19	10	800	252	100
T9	9.43	93.4	5.3	98.7	Fe77B23	10	770	246	152
T23	23.45	93.6	6.0	99.6	Fe75B25	9	820	227	163
T40	40.50	92.2	7.2	99.4	Fe71B29	10	780	219	184
T96	96.35	93.2	6.6	99.8	Fe73B27	6	1370	226	167

spherical, their average sizes can be estimated by the formula

$$\bar{d}(\text{Å}) = \frac{6}{S_{\text{BET}} \cdot \rho} \cdot 10^8$$

where S_{BET} is the BET surface area and ρ the density of the particles. According to the BET surface areas in Table I and using the density of 7.86 g/cm^3 (the density of iron), the average particle diameters of the Fe–B samples prepared with different reaction time are calculated as shown in Table I and Fig. 5. It is seen that the particle size remains at about 800 Å with the reaction time ranging from 5 to 40 min. For the reaction time less than 5 min, the particle size decreases with the addition rate of KBH_4 solution. The sample with the highest addition rate (142 ml/7 sec) has the smallest average particle size of about 590 Å. The sample with the longest reaction time of 96 min in this study has a large average particle size of around 1370 Å. The results were confirmed by the TEM photographs as shown in

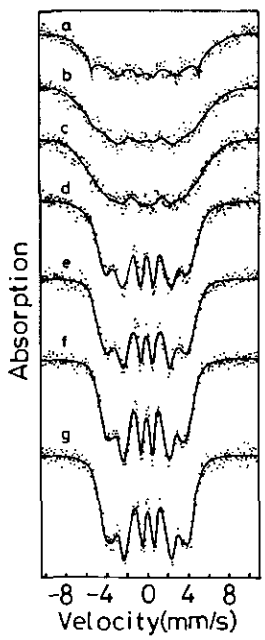

FIG. 3. Room temperature Mössbauer spectra of the Fe–B alloys prepared with the different reaction times: (a) 7 sec, (b) 2.23 min, (c) 5.00 min, (d) 9.43 min, (e) 23.45 min, (f) 40.50 min, and (g) 96.35 min.

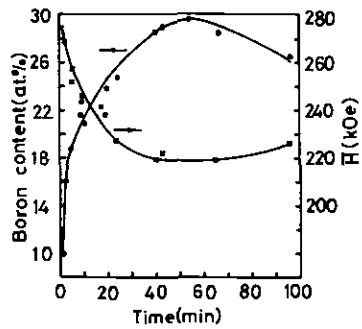

FIG. 4. The dependence of boron content (●) and mean hyperfine field (×) of the Fe–B alloys upon the reaction time used.

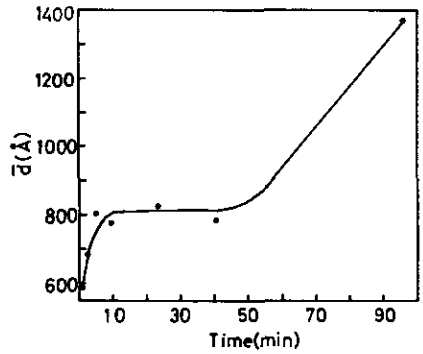

FIG. 5. The dependence of particle size of the Fe–B alloys upon the reaction time used.

Fig. 6. The TEM photographs clearly show that the particles of the T7s sample are small and the particles of the T96 sample are large, but the samples prepared with the reaction time from 5 to 40 min do not have significant differences in particle size. It should be noted that the particles form chains when their sizes are smaller than 800 Å. This may reflect the self-magnetization of the small Fe–B particles in single magnetic domains.

Figure 7 shows the DSC profiles of the Fe–B samples prepared with different reaction times, which also exhibit systematic changes. The exothermic peaks in the DSC profiles are assigned to the crystallization of amorphous phases in the samples. However, other possibilities that the DSC peaks may result from impurities and sintering of small particles in the samples must be excluded. It seems that there is not much heat produced from sintering of the particles during DSC because the samples prepared with the reaction time from 7 sec to 40 min do not have much difference in particle size and the samples prepared with the reaction time longer than 5 min show only one distinct DSC peak. As for impurities, as indicated above, ICP analysis accounts for nearly 100% weight of iron and boron in the samples. The total weight of iron and boron in the T7s sample is 94%, which is lower than 100% and probably balanced by water because the samples were dried by washing with acetone. In another group of test, a sample prepared by the reduction of $FeCl_3$ with very fast addition rate of KBH_4 solution contained 99.5% weight of iron and boron, as analyzed by ICP, and showed the similar Mössbauer spectrum and DSC profile as the T7s sample in this study. Moreover, in our experience, the samples containing impurities that have not washed out usually give some endothermic DSC peaks. Because of these reasons, we suppose that the exothermic peaks in DSC profiles of the Fe–B samples reported here result from the crystallization of amorphous phases. As indicated in our previous work (*18*), the iron atoms with fewer nearest-neighbor boron atoms are less stable than those with more nearest-neighbor boron atoms and will crystallize at lower temperature. So, if there is only one exothermic peak in DSC profile, all iron atoms may have similar number of nearest-neighbor boron atoms, i.e., the boron atoms may be homogeneously distributed throughout the particles, and so forth. The T7s sample prepared with the very fast addition rate (142 ml/7 sec) gives two exothermic peaks with temperatures at 668 and 758 K, respectively. This implies that different amorphous microstructures may exist in this sample (*18*), which is consistent with the result obtained by Mössbauer spectroscopy, where the sample shows a very broadened spectrum with low signal to noise ratio, indicating that the atoms in this sample may be highly disordered and loosely bound to each other. With the increase of reaction time, the peak at lower temperature in the DSC profiles gradually decreases and finally disappears at the reaction time of 5 min, while the peak at higher temperature becomes more symmetric, which may reflect that the distribution of the constituent elements and the microstructure of the Fe–B samples become more uniform with the increase of the reaction time (*18*). In Fig. 8 is plotted a linear correlation between heat of crystallization, as deduced from the areas of DSC profiles, and the boron content in the Fe–B samples. Except for the T7s sample, the heat of crystallization (ΔH_C) in-

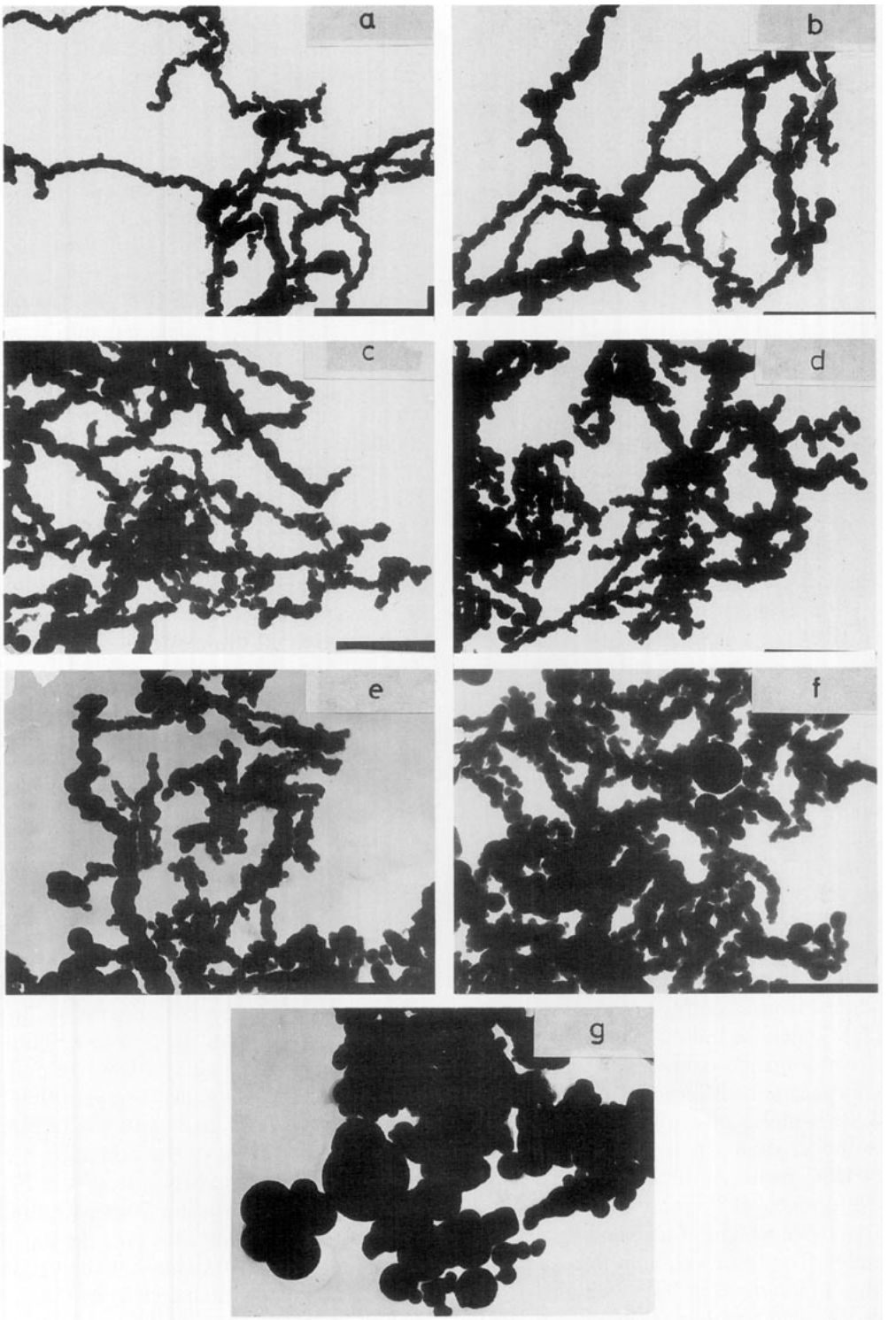

FIG. 6. Transmission electron micrographs of the Fe–B alloys prepared with the different reaction times: (a) 7 sec, (b) 2.23 min, (c) 5.00 min, (d) 9.43 min, (e) 23.45 min, (f) 40.50 min, and (g) 96.35 min. Magnified by 30,000.

creases linearly with the boron content in the Fe–B samples, and the average heat of crystallization, normalized to per mole of boron in the samples, is found to be about 27 kJ. However, the T7s sample with the very fast addition rate (142 ml/7 sec) has much large crystallization heat of about 46 kJ per mole of boron. It seems to support the suggestion that this sample may have more disordered amorphous structure than others.

In conclusion, we have shown that the addition rate of KBH_4 solution into the solution of $FeSO_4$, i.e., the reaction time for the reaction between KBH_4 and $FeSO_4$ in aqueous solution will greatly influence the properties of the Fe–B products in boron content, particle size, and amorphous structures. Therefore, in order to obtain reasonable results in investigating other preparation parameters such as temperature, concentration, molar ratio, etc., the reaction time should always be controlled at a constant value.

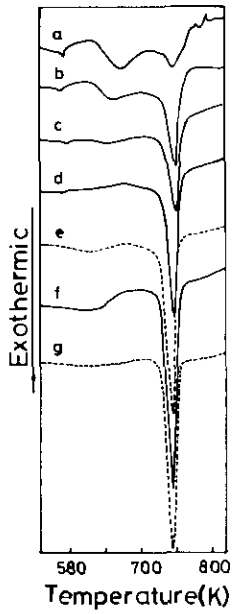

FIG. 7. Differential scanning calorimetric profiles of the Fe–B alloys prepared with the different reaction times (a) 7 sec, (b) 2.23 min, (c) 5.00 min, (d) 9.43 min, (e) 23.45 min, (f) 40.50 min, and (g) 96.35 min.

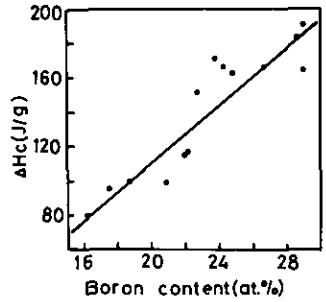

FIG. 8. The heat of crystallization of the Fe–B alloys prepared by chemical reduction as a function of boron content.

Acknowledgment

Financial support from SINOPEC is greatly acknowledged.

References

1. J. VAN WONTERGHEM, S. MØRUP, C. J. W. KOCH, S. W. CHARLES, AND S. WELLS, *Nature* **322,** 622 (1986).
2. S. LINDEROTH, S. MØRUP, A. MEAGHER, J. LARSEN, M. D. BENTZON, B. S. CLAUSEN, C. J. W. KOCH, S. WELLS, AND S. W. CHARLES, *J. Magn. Magn. Mater.* **81,** 138 (1989).
3. Z. HU, Y. HSIA, J. ZHENG, J. SHEN, Q. YAN, AND L. DAI, *J. Appl. Phys.* **70,** 436 (1991).
4. S. LINDEROTH, S. MØRUP AND M. D. BENTZON, *J. Magn. Magn. Mater.* **83,** 457 (1990).
5. S. LINDEROTH, S. MØRUP, C. J. W. KOCH, S. WELLS, S. W. CHARLES, J. VAN WONTERGHEM, AND A. MEAGHE, *J. Phys. Colloq.* **49,** C8-1369 (1988).
6. S. MØRUP, J. VAN WONTERGHEM, A. MEAGHE, AND C. J. W. KOCH, *IEEE Trans. Magn.* **23,** 2978 (1987).
7. J. VAN WONTERGHEM AND S. MØRUP, *Hyper Int.* **42,** 959 (1988).
8. A. INOUE, J. SAIDA, AND T. MASUMOTO, *Metall. Trans. A* **19,** 2315 (1988).
9. A. CORRIAS, G. ENNAS, G. LICHERI, G. MARONGIU, A. MUSINU, G. PASCHINA, G. PICCALUGA, G. PINNA, AND M. MAGIN, *J. Mat. Sci. Lett.* **7,** 407 (1988).
10. S. WELLS, S. W. CHARLES, S. MØRUP, S. LINDEROTH, J. VAN WONTERGHEM, J. LARSEN, AND M. B. MADSEN, *J. Phys. Condens. Matter* **1,** 8199 (1989).
11. J. JIANG, F. ZHAO, P. GAO, I. DEZSI, AND U. GONSER, *Hyper. Int.* **55,** 981 (1990).

12. J. JIANG, I. DEZSI, U. GONSER, AND X. LIN, *J. Non-Cryst. Solids* **124,** 139 (1990).
13. F. S. LI, D. S. XUE, AND R. J. ZHOU, *Hyper. Int.* **55,** 1021 (1990).
14. I. DRAGIEVA, KR. RUSEV, AND M. STANIMIROVA, *J. Less-Common Met.* **158,** 295 (1990).
15. S. LINDEROTH AND S. MØRUP, *J. Appl. Phys.* **67,** 4472 (1990).
16. J. SHEN, Z. HU, Y. HSIA, AND Y. CHEN, *Appl. Phys. Lett.* **59,** 2510 (1991).
17. J. SHEN, Z. HU, L. ZHANG, Z. LI, AND Y. CHEN, *Appl. Phys. Lett.* **59,** 3545 (1991).
18. J. SHEN, Z. HU, Q. ZHANG, L. ZHANG, AND Y. CHEN, *J. Appl. Phys.* **71,** 5217 (1992).
19. S. LINDEROTH AND S. MØRUP, *J. Appl. Phys.* **69,** 5256 (1991).
20. G. LE CAËR AND J. M. DUBOIS, *J. Phys. E. Sci. Instrum.* **12,** 1083 (1979).
21. J. SHEN, Z. LI, Q. YAN, AND Y. CHEN, *J. Phys. Chem.* **97,** in press (1993).